Biology of Reproduction, 2021, 104(5), 1045–1057
doi:10.1093/biolre/ioab020
Research Article
Advance Access Publication Date: 16 February 2021

Research Article

Maternal Cripto is required for proper uterine decidualization and peri-implantation uterine remodeling

Shiva Shafiei[1,2], Omar Farah[1,2] and Daniel Dufort[1,2,3,4,*]

[1]Division of Experimental Medicine, McGill University, Montreal, Canada, [2]Child Health and Human Development Program, Research Institute of the McGill University Health Centre, Montreal, Canada, [3]Department of Obstetrics and Gynecology, McGill University , Montreal, Canada and [4]Department of Biology, McGill University, Montreal, Canada

*__Correspondence:__ Child Health and Human Development program, Research Institute of the McGill University Health Centre, 1001 Blvd. Décarie, CHHD EM03230, Montréal, Quebec H4A 3J1, Canada. Tel: (514) 934-1934 ext. 34743; E-mail: Daniel.dufort@mcgill.ca

†__Grant Support:__ This work was supported by grants from the Canadian Institutes of Health Research PJT-159788 and a March of Dimes grant #21-FY14-130 to D.D. S.S. was supported by a scholarship from the Faculty of Medicine, Division of Experimental Medicine of McGill University and the RI-MUHC.

Received 28 January 2020; Revised 19 November 2020; Accepted 10 February 2021

Abstract

Cripto encodes for a cell surface receptor whose role in embryonic development and stem cell maintenance has been studied. Cripto mRNA and protein have been detected in the human uterus at all stages of the menstrual cycle. To date, there is not much known about Cripto's role in female reproduction. As Cripto null Knockout (KO) is embryonic lethal, we created a conditional KO (cKO) mouse model in which Cripto is deleted only in the reproductive tissues using a Cre-loxP system. Pregnancy rate and number of pups per litter were evaluated as general fertility indices. We observed a significant decrease in pregnancy rate and litter size with loss of uterine Cripto indicating that Cripto cKO females are subfertile. We showed that although the preimplantation period is normal in Cripto cKO females, 20% of cKO females fail to establish pregnancy and an additional 20% of females undergo full litter loss after implantation between day 5.5 postcoitum (d5.5pc) and d8.5pc. We showed that subfertility caused by loss of uterine Cripto is due to defects in uterine decidualization, remodeling, and luminal closure and is accompanied by significant downregulation of Bmp2, Wnt4 and several components of Notch signaling pathway which all are known to be important factors in uterine remodeling and decidualization. Our study demonstrates that Cripto is expressed in the uterus during critical stages of early pregnancy and its deletion results in subfertility due to implantation failure, impaired peri-implantation uterine remodeling and impaired uterine decidualization.

Summary sentence

Cripto is involved in uterine luminal closure and stromal decidualization.

Key words: Cripto, decidualization, implantation, uterine remodeling, Notch signaling.

Introduction

Pregnancy is a crucial component of mammalian reproduction comprised of complex sequential events such as implantation, decidualization, placentation, and eventually parturition. Perturbation of these events can lead to different clinical issues including infertility and pregnancy complications like preeclampsia, intrauterine growth restriction (IUGR), and preterm birth [1–3]. Although the major physiological events associated with reproduction have been characterized, there are still many molecular pathways that have yet to be fully elucidated in order to open new avenues toward overcoming and managing these reproductive issues. In vivo research limitations, especially on subjects related to uterine-embryo interactions in humans, has led researchers to rely primarily on animal models to identify the molecular mechanisms that govern reproduction [1–3].

Several studies have demonstrated the involvement of different transforming growth factor-beta (TGFβ) superfamily members and their related receptors in many fundamental reproductive events including: folliculogenesis and ovulation, preimplantation embryonic development, maternal-embryo communication during implantation, uterine decidualization, placentation, embryo patterning and gastrulation, and reproductive tract morphogenesis and function [4–22].

CRIPTO is a member of the epidermal growth factor-Cripto1 /FRL1/Cryptic (EGF-CFC) protein family that acts as a coreceptor in the TGFβ signaling pathways that involve NODAL, GDF1, and GDF3. Cripto has been shown to play a critical role in embryo development [23, 24] and Cripto null mice are embryonic lethal (between d7.5pc and d10.5pc) because of major gastrulation and heart development defects [25]. In addition to being a coreceptor in the TGFβ signaling pathway, CRIPTO can activate Smad-independent signaling pathways such as PI3K/Akt and MAPK and facilitate signaling through the canonical Wnt/ß-catenin and Notch/Cbf-1 signaling pathways [26]. Through these various mechanisms, Cripto is implicated in: early embryogenesis, embryonic stem cell maintenance, facilitating epithelial-mesenchymal transitions and significantly enhancing tumor cell migration, invasion, and angiogenesis [26]. Cripto may also have a role in female reproduction and pregnancy maintenance. Cripto mRNA is consistently detected in endometrial samples from healthy women during the menstrual cycle [27]. The expression of Cripto is also dysregulated in specific human placental and endometrial pathologies like placenta creta, [28] and endometriosis [29]. The specific role of maternal Cripto in female reproduction and pregnancy still remains elusive as no study has yet been conducted that presents an in-depth analysis of its function in the endometrium. In this study, we utilize a uterine-specific conditional knockout of Cripto to investigate whether Cripto is a key contributing component in physiologic events of mouse pregnancy such as implantation and uterine decidualization. Our results demonstrate that Cripto is expressed in the uterus during critical stages of early pregnancy and its deletion results in subfertility due to implantation failure, impaired peri-implantation uterine remodeling, and impaired uterine decidualization.

Materials and methods

Generation and maintenance of Cripto cKO Mice

Experimental protocols in this study are in accordance with regulations established by the Canadian Council on Animal Care and were reviewed and approved by the Animal Care Committee of the McGill University Health Centre. Wild-type CD1 mice were purchased from Charles Rivers Company. Mice with loxP sites flanking exon 3–5 of the Cripto gene (Cripto floxed/floxed or Cripto *f/f*) on a C57BL6 background were purchased from The Jackson Laboratory (Stock Number: 016539, Strain Name: STOCKTdgf1tm2.2Mms/J). The generation of these mice has been previously described [30]. Progesterone receptor-Cre mice (*Pgr Cre/+*) were generously donated by F.J. DeMayo and J.P. Lydon [30] and maintained on a CD1 background in our lab. Both strains have previously been reported to be healthy and demonstrated normal fertility. *Pgr Cre/+* mice have been used in numerous studies to investigate uterine-specific gene function.

Homozygous Cripto *f/f* females were crossed with heterozygous *Pgr Cre/+* males and the offspring were genotyped by tail snip digestion and polymerase chain reaction (PCR). The Cripto floxed (~300 bp) and Cripto wild-type (178 bp) alleles were amplified by touch-down PCR (94°C 30 s, 58–55°C 30 s, 72°C 30 s) for seven cycles decreasing the annealing temperature 0.5°C in every cycle; then 30 cycles of (94°C 30 s, 55°C 30 s, 72°C 30 s) using the following primers: Forward 5′-TGG TGA TCC AGA GTC ATT GG-3′ and Reverse 5′-GGG GTC ATT CCT CTC CTA GC-3′. The *Pgr-Cre* (550 bp) and *Pgr*-wild-type (300 bp) alleles were amplified by standard PCR (94°C 1 min, 60°C 1 min, 72°C 2 min) for 30 cycles using the following primers: 5′-ATGTTTAGCTGGCCCAAATG-3′; 5′-TATACCGATCTCCCTGGACG-3′; 5′-CCCAAAGAGACACCA-GGAAG-3′.

In the first generation, half of the offspring are heterozygous for both genes (Cripto *f/+ Pgr Cre/+*). The heterozygous males (Cripto *f/+ PgrCre/+*) were crossed with Cripto *f/f* females in order to generate all required genotypes which are: Cripto conditional knockout (Cripto cKO: Cripto *f/f, PgrCre/+*), Cripto conditional heterozygous (Cripto cHet: Cripto *f/+, PgrCre/+*) and control females (Cripto *f/f, Pgr +/+*).

Fertility assessments

To assess fertility, 6–8-week-old virgin females (control, Cripto cHet, and Cripto cKO) were mated with sexually mature fertile wild-type CD1 males. Mating was confirmed by observation of a vaginal plug. The day of vaginal plug observation was considered as day 0.5 postcoitum (d0.5pc) through the whole study. Females were separated from males after mating, kept in individual cages and monitored daily for 3 weeks. A successful pregnancy was defined by birth of live pups. The number of pups per litter and duration of pregnancy were also recorded. In a different approach, 12-week-old females were housed with sexually mature fertile wild-type CD1 males for a period of 5 months (one female and one male in each cage). Cages were monitored regularly, and the number of litters and pups were recorded for every female in the study.

For assessment of different stages of pregnancy, the females were mated with sexually mature fertile wild-type CD1 males, then were sacrificed on specific gestational ages. Uteri were dissected and the gross morphology was assessed, photographs were taken and further required analysis was done.

Embryo flushing and collection

control and Cripto cKO females were mated with sexually mature fertile wild-type CD1 males and the day of vaginal plug was assigned as d0.5pc. Females were sacrificed on d2.5pc and d3.5 pc, intact reproductive tract was dissected (ovaries, oviducts, and uterus). Embryos were flushed and collected from the oviducts on d2.5pc and from the uterine horns on d3.5pc.

Measurements of the conceptus site size

Using ImageJ software, the area of each conceptus site was measured in the photographs taken from whole mount pregnant uteri of control and Cripto cKO females at different timepoints of pregnancy.

Tissue processing, paraffin embedding, sectioning, and H&E staining

Dissected samples were collected in phosphate-buffered saline (PBS), fixed overnight at 4°C in 4% paraformaldehyde (PFA)/PBS or 10% neutral buffered formalin, dehydrated in increasing ethanol series (25%, 50%, 75%, and 100%, 20 min each) and cleared in xylene (2 × 15 min). The tissue was incubated overnight in melted paraffin wax (TissueTek) at 60°C in a vacuum oven then embedded at room temperature, and the blocks were placed on a cold plate for 1 h to solidify slowly then transferred to −20°C freezer overnight before sectioning. Seven-micrometer sections were cut with the Leica RM2145 microtome, mounted on Fisherbrand Superfrost plus slides and dried overnight. Slides were then either used for immunofluorescence, immunohistochemistry (described later) or stained with hematoxylin and eosin (H&E). For H&E staining, slides were deparaffinized in xylenes (2 × 5 min), rehydrated with a decreasing ethanol gradient (100%, 95%, 85%, 75%, 50%, 20%, and water, 2 min each), placed in Harris Modified Hematoxylin solution [Sigma] for 6 min and then washed in running tap water for 10 min. Sections were then decolorized with dipping in 1% acidic alcohol (1–2 s), placed in a 1% sodium bicarbonate bluing agent (3 s), before counterstaining with Eosin [Sigma] for 15 s. The slides were then dehydrated, cleared, and mounted using Permount [Fisher Scientific].

Immunofluorescence staining

As described earlier, uteri (nonpregnant or d0.5pc to d4.5pc pregnant) were dissected, dehydrated, cleared, embedded in paraffin blocks and sectioned. Slides were then washed in xylene (2 × 10 min), rehydrated with a decreasing ethanol gradient (100%, 95%, 85%, 75%, 50%, 20%; 2 min each). Antigen retrieval was done in 10 mM sodium citrate solution (+0.05% Tween 20, pH 6) at 95°C for 20 min. Sections then were permeabilized with PBT (0.2% BSA, 2.5% Triton X-100 in PBS for 15 min), blocked for 1 h at room temperature (10% BSA in PBS) then incubated with the primary antibody, (CRIPTO [Santa Cruz sc-17188; 200 µg/ml; 1:100 dilution]; CD45 [Invitrogen, eBioscience, Catalog # 14-0451-82, 0.5 mg/ml; 1:100 dilution]) at 4°C overnight. Following several washes in 0.1% PBS-Tween 20, slides were incubated with the appropriate secondary antibody for 1 h at room temperature (Alexa Fluor 488, Donkey anti-Goat, Life technologies, 2 mg/ml, 1:300 dilution; Alexa Fluor 488, Goat anti-Rat, Catalog # A-11006, 2 mg/ml; 1:300 dilution). Slides were then washed, counterstained with DAPI (1:5000) and mounted with Mowiol 4–88 [Sigma].

Immunohistochemistry

As described earlier, uteri were dissected, dehydrated, cleared, embedded in paraffin blocks and sectioned. Slides were then washed in xylene (2 × 10 min), rehydrated with a decreasing ethanol gradient (100%, 95%, 85%, 75%, 50%, 20%; 2 min each). Antigen retrieval was done in 10 mM sodium citrate solution (+ 0.05% Tween 20, pH 6) at 95°C for 20 min. Sections then were permeabilized with TBT (0.2% BSA, 2.5% TritonX-100 in TBS for 15 min), blocked for 1 h at room temperature (10% BSA in TBS). Following washes in TBS-0.025% Tween 20 (TBST), slides were incubated with primary antibody: CRIPTO [Santa Cruz, sc-17188; Goat IgG raised against Mouse Cripto; 200 µg/ml; 1:100 dilution], COX2 [Cayman, aa570–598, 100 µg/ml; 1:150 dilution] or PCNA [Santa Cruz, FL-261, 200 µg/ml; 1:100 dilution] at 4°C overnight. After washes with TBST, 0.3% H_2O_2 in TBS was used for blocking endogenous peroxidase activity following by incubation with an appropriate secondary HRP antibody (1:500) for 1 h at room temperature. For antigen visualization, DAB Substrate Kit (Abcam ab64238) was used based on recommended instructions provided by the manufacturer. Then slides were counterstained with hematoxylin solution, Gill no. 2 (Sigma–Aldrich) and mounted with Richard-Allan Scientific™ Mounting Medium (Thermo Fisher Scientific).

To validate the specificity of the Cripto antibody used in our study, the serial sections of the d5.5pc pregnant mouse uterus were subjected to either anti-Cripto primary antibody, nonimmune Goat IgG [Calbiochem, EMD Millipore Corp., Normal Goat IgG, cat # NI02-100UG, 0.1 mg/ml; 1:50 dilution] or no primary antibody, followed by treatment with secondary HRP antibody. We observed prominent signal only when Cripto antibody + secondary HRP antibody was used confirming the specificity of the observed signals (Supplementary Figure S7).

Artificial decidualization

control and Cripto cKO females were mated with vasectomized males. On d3.5pc, females were anesthetized with isoflurane and an incision was made on the lower back of the mice lateral to the midline, exposing the ovary and uterus on one side. One uterine horn was subsequently scratched along the uterine lumen on the antimesometrial side with a 22G needle inserted from the proximal end of the uterine horn close to the oviduct. The other horn served as an internal control. The incision was sutured, and females were allowed to recover till d7.5pc when they were sacrificed, and the uterus was dissected out in order to assess the decidualization response.

Alkaline phosphatase staining

After tissue processing, paraffin embedding and sectioning, slides were deparaffinized in xylene (2 × 5 min each) then rehydrated in a series of decreasing ethanol dilutions (100%, 100%, 95%, 75%, 50%, and dH_2O, 2 min each). Slides were preincubated overnight in 1% $MgCl_2$ in Tris-maleate buffer (100 mM Tris-Maleate, 150 mM NaCl, and 1 mM $MgCl_2$, pH 9.2) at room temperature. Slides were incubated for 2 h in alkaline phosphatese-substrate solution at room temperature (NBT 660 µl and 330 µl BCIP in 100 ml Tris-maleate buffer). Slides were then washed, counterstained with nuclear fast red, dehydrated with series of increasing ethanol dilutions, cleared with Xylene, mounted, and imaged.

Hormone analysis

control and Cripto cKO females were mated with sexually mature fertile wild-type CD1 males. On d7.5pc females were euthanized, blood was collected by cardiac puncture, uteri were dissected, and the pregnancy status and number of implantation sites were recorded. Serum was separated from the blood and stored at −80°C prior to being sent to Ligand Assay and Analysis Core at University of Virginia (Charlottesville, Virginia) for hormone analysis where serum Progesterone levels were measured.

Reverse transcription and real-time PCR

RNA extraction was done using Trizol and RNeasy Mini Kit [Qiagen Cat. No. 74104]. QuantiTect Reverse Transcription Kit [Qiagen Cat.

No. 205311] was then used for cDNA synthesis. Real-time PCR was performed using the Rotor-Gene SYBR Green PCR Kit [Qiagen Cat. No. 204074] following the manufacturer's protocol using Corbett Rotor-Gene 6000 thermocycler and the analysis was done using the Rotor-gene 6000 software. The following primers were designed using NCBI primer-blast tool and were checked for the specificity using the tool's blasting feature: Cripto (200 bp) 5′- GACCAGAAAGAACCTGCCGT −3′ and 5′-AGGATAGACCCACAGTGCTCTT −3′; Hoxa10 (207 bp) 5′-CGCTACGGCTGATCTCTAGG-3′ and 5′-CAGCCCCTTCAGAAAACAGT-3′; Hoxa11 (285 bp) 5′-TATAAGGGCAGCGCTTTTTG-3′ and 5′-ACCTCGCTTCCTCCGACTAC-3′; Wnt4 (243 bp) 5′-AACGGAACCTTGAGGTGATG-3′ and 5′-TCACAGCCACATTCTCCAG-3′; Bmp2 (95 bp) 5′-AACACTAGAAGACAGCGGGTC-3′ and 5′-CTCTCTCAATGGACGTGCCC-3′; Notch4 (194 bp) 5′-TTGGCTGAGCAGAAGTCTCG-3′ and 5′-CCTCACTTCTCCTGCACCTG-3′; Notch1 (371 bp) 5′-TCACTCTCACAGTTGCGACC-3′ and 5′-AGTGGCCCTAATTGCCAGAC-3′; Dll4 (149 bp) 5′-TTCTTGCACGGAGAGTGGTG-3′ and 5′-CAACACGACACCGGAACAAAC-3′; GAPDH (223 bp) 5′-AACTTTGGCATTGTGGAAGG-3′ and 5′-ACACATTGGGGGTAGGAACA-3′; Ihh (196 bp) 5′- CTACAAGCAGTTCAGCCCCA-3′ and 5′- TGAGTTCAGACGGTCCTTGC-3′; Cox2 (232 bp) 5′- GCTGTACAAGCAGTGGCAAA-3′ and 5′-CCCCAAAGATAGCATCTGGA −3′.

The efficiency of every primer set was validated by creating a standard curve using series dilutions of a good quality cDNA (five dilutions by a factor of 10). The results from the qPCR machine were then used to create a standard curve, where the slope and R2 values were calculated to determine the efficiency of the primers. All primers used in this study had an efficiency >95% as judged by the standard curve analysis. Subsequently, only primers with this efficiency or higher were used to calculate relative expression of the respective gene of interest by using the ΔΔCT method where we obtained the fold changes in gene of interest expression normalized to an internal control gene (Gapdh), and relative to one line (calibrator). In every qPCR run, melt curve analysis was performed to confirm the presence of a single peak.

Statistics

Data are presented as the mean ± standard error of the mean of independent samples. Statistical analysis comparing experimental groups was performed using two-tailed Student *t*-test for independent samples, Student *t*-test for correlated samples and one-way ANOVA followed by a Tukey's multiple comparison test. *P*-values less than 0.05 were considered statistically significant.

Results

CRIPTO is present in the uterus during the peri-implantation and early postimplantation periods

To determine the spatiotemporal localization of CRIPTO in the wild-type mouse uterus, we performed immunofluorescence staining against CRIPTO in nonpregnant and peri-implantation stages of pregnancy (d0.5pc-d4.5pc). CRIPTO was sparsely observed in the nonpregnant uterus with a slight increase after mating (d0.5pc) (Supplementary Figure S1). Protein levels significantly increased from d2.5pc onward and was prominently localized in uterine stromal cells (Supplementary Figure S1).

To further characterize the pattern of CRIPTO localization during early pregnancy, immunohistochemistry was also performed on d1.5pc, d3.5pc, and d5.5pc uteri. On d1.5pc limited CRIPTO localization was only observed in a few stromal cells adjacent to the luminal epithelium and in a few cells within the luminal epithelium. Other compartments of uterus did not show any CRIPTO localization at this timepoint (Figure 1A and B). Interestingly, on d3.5pc, CRIPTO levels became quite prominent in the embryo (Figure 1C and C″) as well as in the subluminal uterine stroma and luminal epithelium only at the future implantation sites and not at the interimplantation spaces (Figure 1C–D″). A gradient pattern of CRIPTO localization in the stromal cells at the implantation site was also observed where it was mostly visible in the stromal cells adjacent to the luminal epithelium and decreased with distance away from the lumen toward the periphery of the uterus (Figure 1C–C″).

Our immunohistological evaluations on d5.5pc (1 day after implantation) revealed that similar to d3.5pc, localization of CRIPTO is limited to the implantation sites. At this timepoint, CRIPTO was observed in decidual cells and differentiating stromal cells (Supplementary Figure S2).

Immunohistological evaluations on d3.5pc and d5.5pc also revealed perivascular localization of CRIPTO in pregnant uteri. This localization was very prominent around the mesometrial vasculature (Supplementary Figure S3A and C) and although present, showed less intensity around the vascular structures in myometrium and stroma (Supplementary Figure S3B and D). This perivascular localization of CRIPTO was not limited to implantation sites as it was also visible in interimplantation spaces.

Cripto conditional knockout females are subfertile

Cripto null mutants are embryonically lethal, therefore, a tissue-specific conditional knockout (cKO) of Cripto in the maternal reproductive tract using a Cre-loxP recombinase system was employed. The Cre-recombinase in this mouse model is driven under the progesterone receptor (PR) promoter, thereby creating a specific deletion of Cripto in female reproductive tissues (Figure 2A). Gross morphology and histology of the uterus in Cripto cKO mice was observed to be normal. By means of IHC, CRIPTO deletion was confirmed by its absence on d3.5pc at the implantation sites where CRIPTO localization is expected in the luminal epithelium and stromal cells (Figure 2B–C′). Interestingly, as expected, CRIPTO was still detected in the embryo at this stage (Figure 2C′). On d5.5pc, CRIPTO was also absent in decidual cells and differentiating stromal cells (Figure 2D–E′).

To assess fertility, we mated 6–8-week-old virgin Cripto conditional heterozygous (Cripto cHet), Cripto cKO, and control females with proven fertile wild-type CD1 males and plugged females were included in the study. A successful pregnancy was defined by delivery of live pups after the recorded mating. In this trial, only 62% of mated Cripto cKO females gave birth to pups which was significantly lower than Cripto cHet (94%) and control (100%) females ($P < 0.05$) (Table 1). Furthermore, in this trial, a slightly but statistically significant lower number of pups per litter was observed in Cripto cKO females as compared to cHet and controls (7.68 pups/litter in cKO versus 9.52 in cHets and 9.71 in control; $P < 0.05$) (Table 1). As Cripto cHets mice showed similar fertility parameters to Controls, we continued our study only with Cripto cKO and control mice.

In order to identify the reason for the lower pregnancy rate in young Cripto cKO females, we first examined cycling, ovulation, and fertilization and did not observe any difference between Cripto cKO and controls (data not shown). We next examined the embryos

Table 1. Overall and preimplantation fertility assessment in Cripto cKO versus control females

	Cripto control	Cripto cKO	Cripto cHet
Overal fertility rate (%)	100% (seven of seven)	62.5% (15 of 24)	94.4%(17 of 18)
No. of pups/litter	9.71 ± 0.36	7.68 ± 0.59	9.52 ± 0.62
Percent of plugged mice with embryos on d2.5pc	100% (10 of 10)	100% (7 of 7)	NA
No. of embryos/dam retrieved on d2.5 pc	10.3 ± 0.73	9.28 ± 0.86	NA
Percent of plugged mice with embryos on d3.5pc	100% (nine of nine)	100% (10 of 10)	NA
No. of embryos/dam retrieved on d3.5 pc	7.22 ± 0.7	7 ± 0.78	NA

Table 2. Assessment of pregnancy status on d5.5pc and d8.5pc in Cripto cKO versus control females

	d5.5 pc		d8.5 pc	
	Cripto control	Cripto cKO	Cripto control	Cripto cKO
Pregnancy rate	100% (nine of nine)	78.5% (11 of 14)	100% (five of five)	50% (5 of 10)
No. of mice with implantation failure	0 (0%)	3 (21.43%)	0 (0%)	2 (20%)
No. of mice with full litter resorption	NA	NA	0 (0%)	3 (30%)
No. of implantation sites/pregnant mouse	10.56 ± 0.5	10.27 ± 0.72	9.8 ± 0.2	9.75 ± 0.62
No.of resorption sites/pregnant mouse	0	0	0.4 ± 0.4	1.5 ± 0.64
Decidual area (mm^2)	NA	NA	13.89 ± 0.25	13.69 ± 0.3

isolated at d2.5pc and d3.5pc. A similar number of embryos were retrieved from Cripto cKO and control groups (Table 1) and no morphological differences were observed between embryos from either group (data not shown). To evaluate the postimplantation period, Cripto cKO and control females were sacrificed on d5.5pc and d8.5pc for the assessment of their pregnancy status. Females with visible implantation sites were considered as pregnant. The number of implantation sites (decidua), average decidual size, number of resorption sites and incidence of full litter resorption was compared between groups (Table 2). Our assessments showed that although around 60% of Cripto cKO females established pregnancy and had similar fertility parameters with control females until d8.5pc (Table 2 and Figure 3A), approximately 20% of Cripto cKO females never establish pregnancy, showing no signs of any decidua, even though a mating plug was observed and corpora lutea (CLs) were present on their ovaries (data not shown). Furthermore, an additional 20% of Cripto cKO females established pregnancy but failed to maintain their pregnancy and lost their entire litter between d5.5pc and d8.5pc (Table 2 and Figure 3A). The loss of pregnancy between these timepoints may be the result of delayed implantation which may have compromised pregnancy of Cripto cKO mice, especially those females which lose their entire litter. Together, these two latter groups contributed to the observed overall 40% infertility in young Cripto cKO females. To assess the possibility of implantation failure, the uteri of d5.5pc mated but nonpregnant Cripto cKO females were processed and embedded in paraffin blocks. Serial sectioning and H&E staining were done, and the slides were analyzed using bright-filed microscopy. No sign of embryo attachment/implantation and decidualization initiation was observed (data not shown) confirming implantation failure in these mice.

Uterine decidualization is compromised in Cripto cKO females

The pattern of CRIPTO localization and findings on early pregnancy failure in Cripto cKO females suggested that Cripto might play a role in the process of decidualization during the early stages of pregnancy. We therefore performed artificial decidualization within a single uterine horn of pseudopregnant Cripto cKO and control females and used the contralateral horn as the internal control. Interestingly, all control females responded and significant decidualization was observed in the induced uterine horn, whereas none of the Cripto cKO females had any response (Figure 3B and C). This result suggests that Cripto is involved in the process of decidualization. Although Cripto cKO females have no response to artificial signal for decidualization (mechanical trauma exerted by the needle scratch), they mostly show decidualization (although compromised) when they are bred by fertile males and therefore are subjected to both mechanical (embryo penetration into the uterine wall) and biochemical (signaling molecules originating from the embryo) triggers of decidualization.

As progesterone (P4) from the ovaries is the major regulator of uterine receptivity as well as initiation and maintenance of uterine stromal decidualization, we evaluated the level of progesterone in blood circulation of Cripto cKO females and compared them to Controls. No difference in the level of circulating progesterone was observed between d7.5pc control and Cripto cKO females (including all three categories described earlier) and all animals had the minimum required concentration of blood P4 for that gestational age (Supplementary Table S1) [31].

Looking for the cause of compromised decidualization ability in Cripto cKO females, we evaluated the expression level of some of the important factors known to affect uterine decidualization including *Ihh, Cox2*, *Hoxa10, Hoxa11, Wnt4*, *and Bmp2* [1] in d5.5pc pregnant control, d5.5pc pregnant Cripto cKO and d5.5pc nonpregnant Cripto cKO mice. Although the expression of *Ihh, Cox2, Hoxa10*, and *Hoxa11* showed no difference between groups (Supplementary Figure S4), the expression of *Bmp2* and *Wnt4* was significantly lower in d5.5pc nonpregnant Cripto cKO mice compared to the pregnant d5.5pc cKO and Controls. The expression of *Wnt4* was also significantly lower in pregnant d5.5pc cKO compared to pregnant d5.5pc Controls (Figure 3D and E). To assess whether P4 supplementation can improve the pregnancy rate, Cripto cKO

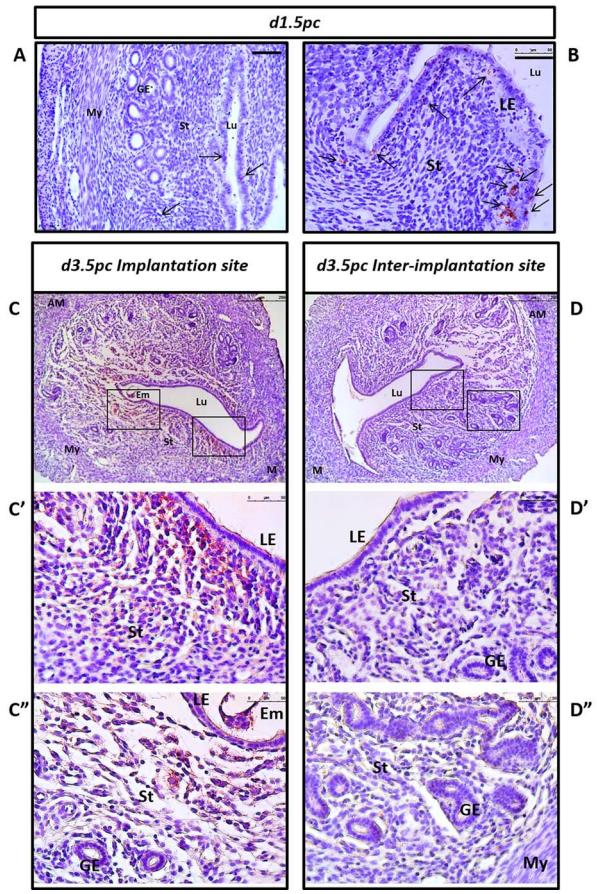

Figure 1. Cripto localization in pregnant uterus corresponds with implantation sites. Localization of Cripto (brown) is shown by immunohistochemistry. On d1.5pc, CRIPTO expression (arrows) is very low and is limited to a few stromal cells adjacent to the luminal epithelium and in a few cells within the luminal epithelium (A and B). On d3.5pc, CRIPTO expression is quite prominent in the uterine stromal cells and to a less extent in the luminal epithelium only at future implantation site (C, C′, and C″) but not at interimplantation space (D, D′, and D″, sections are from the same pregnant uterus). Gradient pattern of CRIPTO expression in the stromal cells at the implantation site is also noticeable (C–C″) where the expression is highest in the stromal cells adjacent to the luminal epithelium and decreases with distance from the luminal epithelium toward the periphery of the uterus. CRIPTO expression is also visible in the embryo within uterine lumen (C″). C′, C″, D′, and D″ are higher magnification of the fields defined by boxes in C and D. AM, antimesometrial pole; Em, embryo; GE, glandular epithelium; LE, luminal epithelium; Lu, lumen; M, mesometrial pole; My, myometrium; St, stroma. Images are representative of ≥3 independent samples for each timepoint. Negative control sections subjected to dilution buffer with no primary antibody displayed no positive staining (images not presented) (Scale bar: A, 75 μm; B, C and D, 50 μm; C′, C″, D′, and D″, 250 μm).

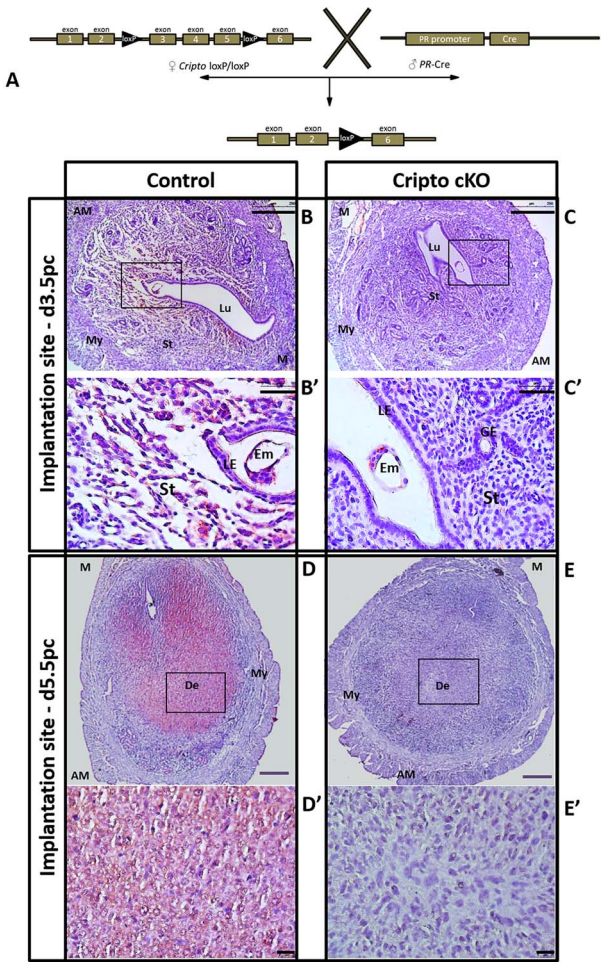

Figure 2. Conditional deletion of Cripto in the mouse uterus. The Cre-recombinase is driven under the progesterone receptor (PR) promoter, thereby creating a specific deletion of Cripto in reproductive tissues of mice bearing loxP insertions before exon 3 after exon 5 of Cripto gene (A). By IHC, Cripto deletion was confirmed in the implantation sites where Cripto localization (brown) is expected in luminal epithelium and stromal cells on d3.5pc (B-C′) and in decidual cells and differentiating stromal cells on d5.5pc (D-E′). In B′, although there is no sign of Cripto expression in the uterus, the localization of Cripto in the embryo present within the uterine lumen is quite evident which further confirms the successful deletion if Cripto in the maternal tissues. B′, C′, D′, and E′ are higher magnification of the fields defined by black boxes in B, C, D, and E respectively. Images are representative of ≥3 independent samples for each timepoint. Negative control sections subjected to dilution buffer with no primary antibody displayed no positive staining (images not presented) AM, antimesometrial pole; De, decidual cells; Em, embryo; GE, glandular epithelium; LE, luminal epithelium; Lu, lumen; M, mesometrial pole; My, myometrium; St, Stroma. (Scale bar: B, C, D, and E: 250 μm; B′ and C′: 50 μm; D′ and E′: 25 μm).

females were mated with fertile wild-type CD1 males and on d3.5pc half of them were supplemented with subcutaneous P4 implants. On d7.5pc, mice were sacrificed, and pregnancy status was determined based on observation of decidua. No difference was observed between the two groups suggesting that P4 supplementation cannot compensate for the lack of uterine CRIPTO in terms of pregnancy rate (data not shown).

In order to evaluate the differentiation status of decidualizing stromal cells in pregnant Cripto cKO females versus controls, alkaline phosphatase (ALP) staining was performed on histological sections of d5.5pc implantation sites. Interestingly the level of ALP activity was drastically lower in Cripto cKO females compared to Controls indicating compromised differentiation of decidual cells in the former group (Figure 3F).

Abnormal implantation crypt and incomplete uterine luminal closure in pregnancy of Cripto cKO females

During the peri-implantation period, proper remodeling of uterine lumen and stroma is critical for successful implantation. This process

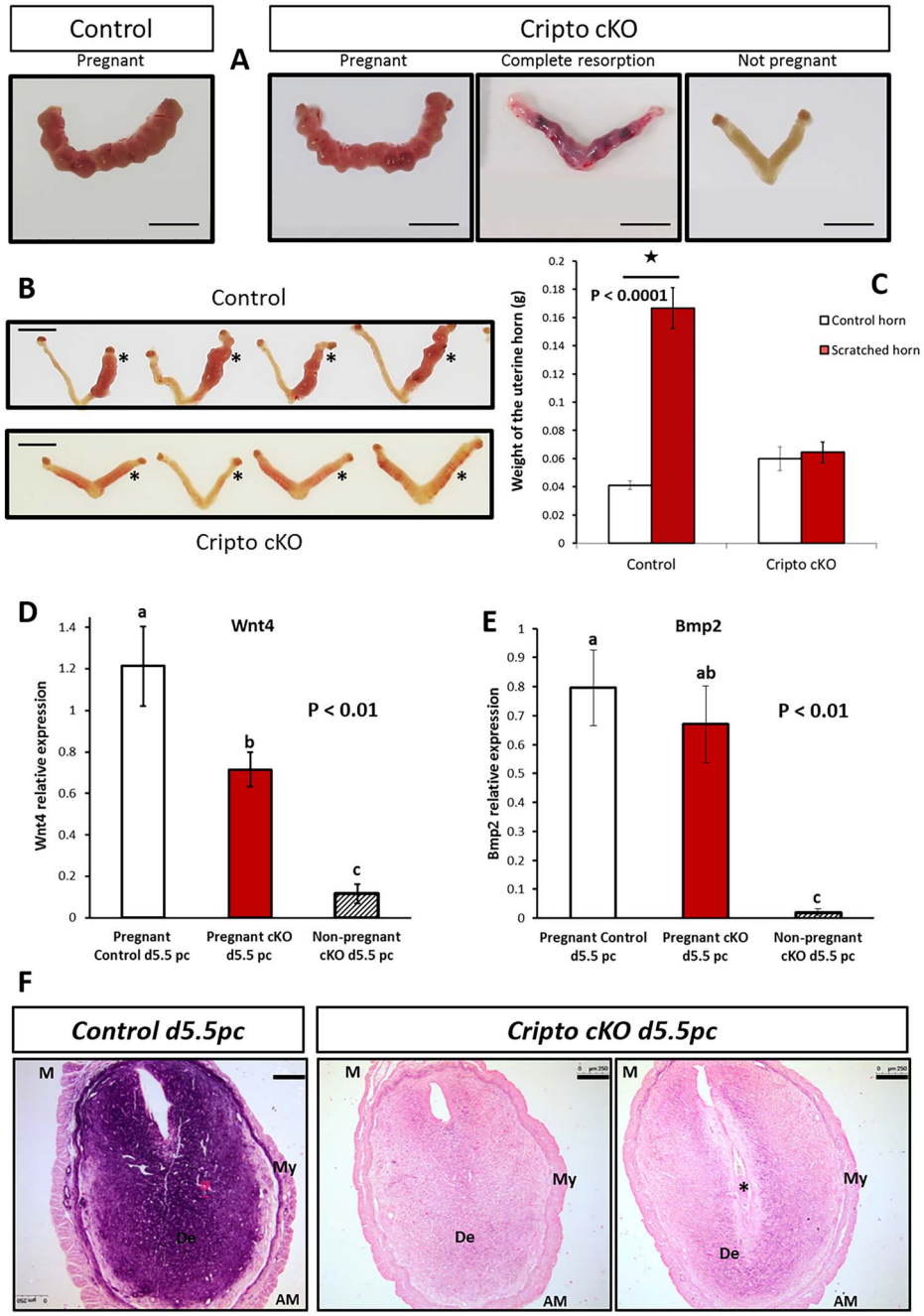

Figure 3. Impaired decidualization in Cripto cKO females. (A) On d8.5pc Cripto cKO females are either pregnant (left image) with pregnancy parameters comparable to control group, or they have established pregnancy but have gone through full litter loss (middle image) or have failed to established pregnancy at all (right image)(*n* for each group is presented in Table 2. (B) Uterine decidualization ability was assessed by artificial induction of decidualization in pseudopregnant females on d3.5pc. whereas all control females (9 of 9) positively responded to this experiment by decidualization of the scratched uterine horn, none of the Cripto cKO females (0 of 9) had any response. (C) The decidualization response was also quantified by comparing the weight of scratched horn (marked by star) versus nonscratched horn (internal control) on d7.5pc which was 4 days after the procedure. (D and E) Relative expression level of *Wnt4* and *BMP2* on d5.5pc was measured by quantitative real-time PCR (pregnant control d5.5pc, $n = 6$–8 females; pregnant Cripto cKO d5.5pc, $n = 8$–10 females and nonpregnant Cripto cKO d5.5pc, $n = 5$–6 females). (C, D, and E) *P*-values for significant differences are included in each panel and different letters or asterisks define the groups which are significantly different. (F) Alkaline phosphatase (ALP) staining and nuclear fast red counterstain on d5.5pc implantation sites. High levels of ALP activity in decidual cells in control females resulted in development of strong purple color whereas the staining is very weak in the case of Cripto cKO females. Images in panel F are representative of ≥3 independent samples. AM, antimesometrial pole; De, decidual cells; M, mesometrial pole; My, myometrium; embryo in the section is marked by star (Scale bar: 250 μm).

starts around d3.5pc and results in formation of single longitudinal implantation crypt which is oriented along the antimesometrial/mesometrial (AM/M) axis of the uterus. The embryo implants at the AM pole of the implantation crypt. With the start of the implantation process, decidualization and remodeling of decidualizing stroma leads to complete closure of the uterine lumen at the implantation sites and is critical for proper placentation later in the course of pregnancy [3]. Abnormal implantation crypt on d3.5pc (irregular shape with presence of extra branch versus the expected single longitudinal AM/M oriented crypt (Figure 2B and C; Supplementary Figure S5A and B) and incomplete luminal closure on d4.5pc and d7.5pc (Figures 4A–D and S5C–E) were observed in histological analysis of the implantation sites in Cripto cKO females but not the controls, suggesting impaired remodeling of uterine lumen and stroma in the former group.

Notch signaling pathway components are known to be involved in uterine luminal closure and stromal remodeling during decidualization [17, 32, 33] and Cripto has been shown to modulate the activity of this pathway [34]. Considering disrupted Notch signaling as a possible cause of the observed impaired uterine remodeling in Cripto cKO females, the expression of components of Notch signaling pathway in the uteri of pregnant Cripto cKO and control mice was assessed on d5.5pc. Interestingly we observed that the expression of *Notch1*, *Notch4*, and *Dll4* are significantly lower in Cripto cKO females compared to Controls (Figure 4E). Thus, Cripto cKO females have reduced expression of Notch receptor and ligand which can account for the observed disruption in luminal closure and stromal remodeling in pregnancy of these mice.

We evaluated the proliferative status of stroma and luminal epithelium on d3.5pc and d4.5pc using IHC against proliferative cell nuclear antigen (PCNA) (Supplementary Figure S5). On d4.5pc, strong PCNA staining in uterine stromal cells of Cripto cKO females indicates high level of proliferation showing that proliferation of uterine stromal cells is not compromised (Supplementary Figure S5).

Fertility of Cripto cKO females declines drastically by age

To understand whether loss of uterine Cripto could have any age-associated deteriorative effects on fertility, we followed the fertility of 6–8-week-old Cripto cKO and Controls females over a period of 5 months and observed a drastic decline in fertility of Cripto cKO females by age in contrast to Controls. Briefly, four Cripto cKO and four control females were caged individually with fertile wild-type males and were monitored regularly. At the end of this trial, the four control females totally gave birth to 219 pups from 21 litters where Cripto cKO females together gave birth to only 101 pups from 19 litters. Although after 5 months of breeding, the average number of litters per female was not different between groups (5.25 ± 0.75 litters/control female versus 4.75 ± 0.25 litters/Cripto cKO female) but the average number of pups per litter was significantly lower ($P < 0.0001$) in Cripto cKO group (5.32 ± 0.64 pups/litter) compared to control group (10.42 ± 0.54 pups/litter) (Figure 5A). Another interesting observation was the obvious decline in the average number of pups per litter over time in Cripto cKO females in contrast to control females where they showed a rather consistent number of pups per litter over 5 months of breeding trial (Figure 5B).

To better understand the nature of the observed age-associated fertility deterioration in Cripto cKO females, we asked whether this decline in fertility could be the adverse effect of repeated pregnancy failure/complications on the uterine structure. Therefore, old virgin (7–8 months old) Cripto cKO ($n = 7$) and Controls ($n = 7$) females were mated with wild-type fertile males. Cripto cKO females were completely infertile and did not give birth to any pups after two rounds of successful mating whereas the age-matched virgin Controls were fertile and produced total of 63 pups (Supplementary Table S2). Further analysis showed although the old Cripto cKO females mate at a similar rate to controls and have similar number of CLs per ovary with control females (6.33 ± 0.81 CLs/ovary in control versus 5.08 ± 0.65 CLs/ovary in Cripto cKO females, Supplementary Table S2 and Figure 6A and B), the number of viable blastocysts (i.e., with normal appearance and developmental stage) retrieved from their uterus on d3.5 postcoitum was less than half of those retrieved from the control females (4.83 ± 2.22 blastocysts/mated control female versus 1.71 ± 0.68 blastotysts/mated Cripto cKO female, Supplementary Table S2, statistically not significant). Histology and immunofluorescence staining (Figures 6C–F and S6) on d3.5pc uteri of these old Cripto cKO females showed the presence of distended endometrial glands (in six out of seven females) and considerable infiltration of immune cells into the lumen of uterine glands (in four out of seven females) in contrary to their aged-matched Controls ($n = 5$). These findings suggest an aberrant immune reaction within the aged uterus possibly associated with loss of uterine Cripto, making the uterine environment unfavorable for blastocysts survival and implantation leading to infertility of Cripto cKO females by progress of the age.

Discussion

Currently, how Cripto is involved in female reproduction is not well understood. In our study, we have shown that Cripto is expressed in the uterus during critical stages of early pregnancy and its deletion results in subfertility due to of implantation failure, impaired peri-implantation uterine remodeling, impaired uterine decidualization, and possibly delayed implantation.

Most of the literature concerning the mechanisms by which Cripto influences gene expression and cellular processes comes from studies of the Nodal signaling pathway. Nodal signal is mediated by binding to an extracellular membrane-bound receptor complex comprised of type I (ALK4/ALK7, mainly ALK4) and type II (ActRIIA/ActRIIB) Activin receptors, along with an EGF-CFC coreceptor (Cripto/Cryptic, mainly Cripto). Activation of the receptor complex results in phosphorylation of the transcription factors SMAD2 and SMAD3. Phosphorylated SMAD2/3 binds to SMAD4, which allows for the nuclear translocation of the SMAD2/3/4 complex. These SMADs then associate with additional transcription factors, such as FoxH1, Mixer, and p53 to facilitate DNA binding and regulation of downstream target genes [35]. It is known, however, that besides being a coreceptor for Nodal, Cripto can activate Smad-independent signaling elements such as PI3K/Akt and MAPK and also facilitate signaling through the canonical Wnt/ß-catenin and Notch/Cbf-1 pathways by functioning as a chaperone protein for LRP5/6 and Notch, respectively [26].

Among the components of Nodal-Cripto-Alk4-Smad dependent pathway, the uterine expression pattern and/or reproductive consequences of uterine deletion of Nodal [11, 12], ALK4 [19], Smad3 [13], Smad2, and Smad4 [21, 36] have been studied. Deletion of Cripto in the female reproductive tract does not phenocopy uterine-specific deletion of Nodal or Alk4. Some physiologic events are disrupted in Nodal cKO mice but seem to be normal, impaired

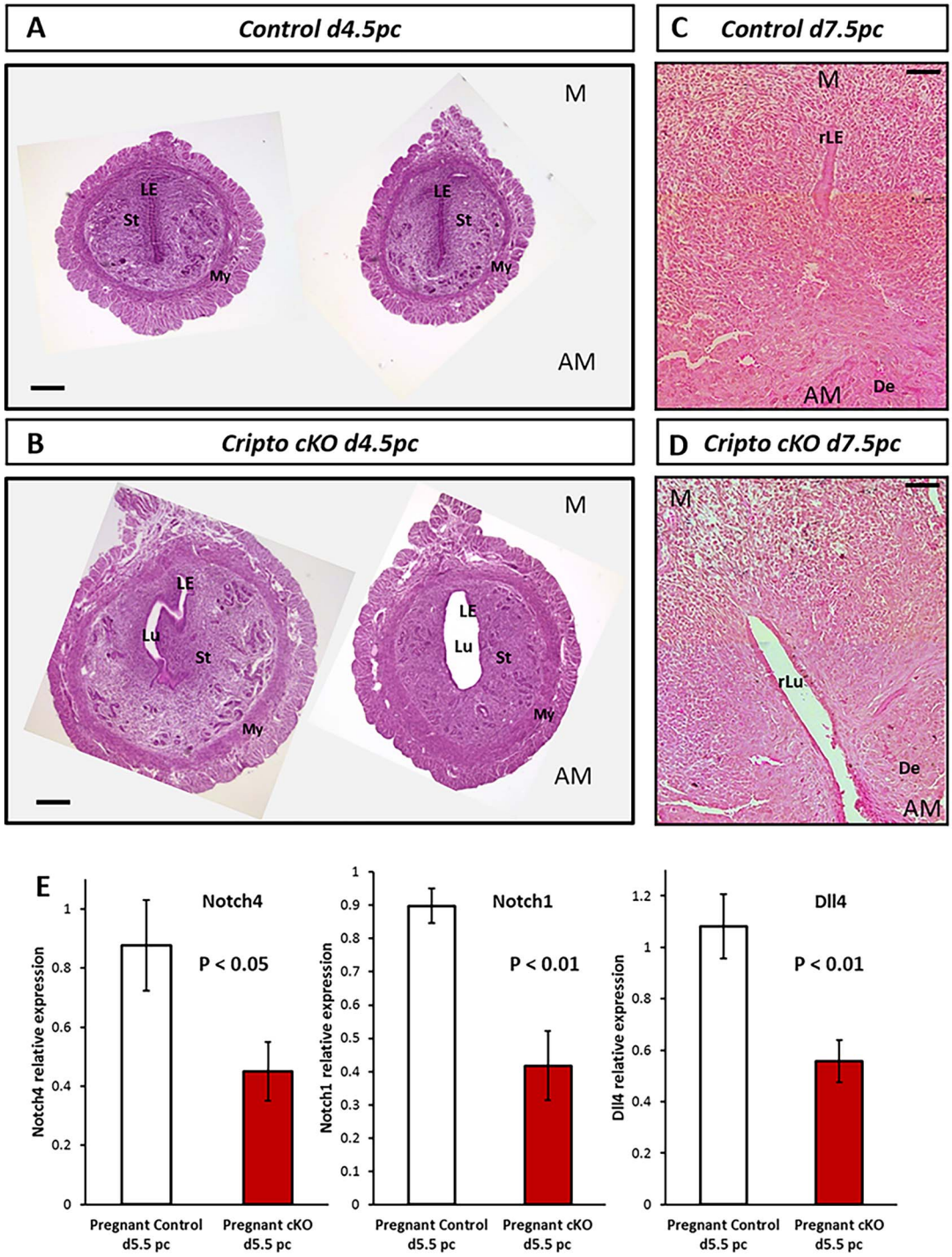

Figure 4. Failure of implantation associated uterine luminal closure in Cripto cKO females accompanied by downregulation of Notch signaling components. Hematoxylin and eosin (H&E) stained sections from d4.5pc (A–B) and d7.5pc (C–D) implantation sites in Cripto cKO females and Controls. On d4.5pc in control group, uterine lumen in implantation sites is completely closed in contrast to cKO females. On d7.5pc, in implantation site of control uterus, residues of closed uterine lumen can be seen whereas in many implantation sites from Cripto cKO females, failure of uterine luminal closure is still quite evident. Images are representative of ≥3 independent samples for each timepoint. (E) Relative expression level of Notch4, Notch1, and Dll4 on d5.5pc was measured by quantitative real-time PCR (pregnant control d5.5pc, $n = 6$–8 females and pregnant Cripto cKO d5.5pc, $n = 8$–10 females). *P*-values for significant differences are included in each panel. AM, antimesometrial pole; De, decidual cells; LE, luminal epithelium; Lu, lumen; M, mesometrial pole; My, myometrium; rLE, residual luminal epithelium; rLu, residual lumen; St, Stroma (Scale bar, d4.5pc: 250 μm; d7.5pc: 75 μm).

with less severity or impaired with a different phenotype in Cripto cKO and/or Alk4 cKO mice. A conditional deletion of Nodal in the mouse uterus, using a similar loxP-Cre system, resulted in a dramatic reduction in fertility of Nodal conditional homozygous knockout

A

	Control females (n=4)	Cripto cKO females (n=4)
Total no. of pups-first month	32 pups/4 litter	10 pups/1 litter
Total no. of pups-second month	35 pups/3 litters	48 pups/7 litters
Total no. of pups-third month	55 pups/5 litters	22 pups/4 litters
Total no. of pups-forth month	55 pups/5 litters	7 pups/2 litters
Total no. pups-fifth month	42 pups/4 litters	14 pups/5 litters
Total no. of pups over 5 months	219 pups	101 pups
Total no. of litters over 5 months	21 litters	19 litters

B

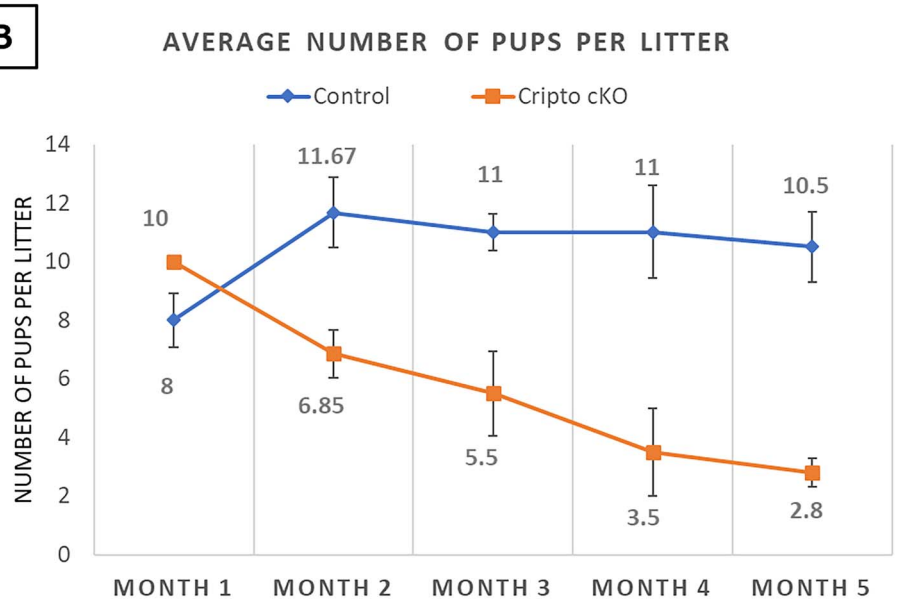

Figure 5. Assessment of fertility in a 5 months-long breeding trial. (A) The number of pups and litters produced by control and Cripto cKO females during every month of the trial. (B) Average number of pups per litter over time is shown in Cripto cKO females compared to Controls.

and conditional heterozygous females due to impaired implantation, decidualization, and placentation [12]. Unlike Cripto cKOs and Alk4 cKOs however, Nodal cKOs are prone to preterm delivery on d17.5pc as opposed to term birth at d19.5pc [12] and both Nodal cKO and Nodal cHet females showed significantly higher sensitivity to infection-induced inflammation which causes them to deliver prematurely [4]. Even though ovulation, fertilization, and early embryo development are normal in Cripto, Nodal, and Alk4 cKO mouse models, considerable implantation failure is observed in Nodal cKO mice; this phenotype is very mild in Cripto cKO and Alk4 cKO females however [19]. This observation can be justified with these two possibilities: (1) Nodal role in regulating implantation is exerted through Cripto/Alk4/Smad-independent pathways and/or (2) Nodal target cells in the uterus during peri-implantation period are those that do not express progesterone receptor (most probably immune cells); Therefore, Cripto or Alk4 would not be deleted in these cells and the required pathway will remain active.

Comparative analysis of decidualization in Nodal, Cripto, and Alk4 conditional KO female mice suggests that Nodal and Cripto, but not Alk4, are required for stromal decidualization. Evaluated by means of artificial decidualization, whereas both Cripto cKO (shown in the present study) and Nodal cKO females (Park CB, Dufort D; manuscript in preparation) show a compromised decidualization ability in response to artificial trigger of decidualization, Alk4 cKO females reveal no defect in decidualization as they react completely similar to control females [19]. This observation can suggest that Nodal and Cripto are involved in uterine decidualization probably through Alk4/Smad-independent pathways.

We have assessed the level of some critical factors in uterine decidualization including the serum level of progesterone (P4) on d7.5pc and expression of Cox2, Ihh, Hoxa10, Hoxa11, Bmp2, Wnt4, and Notch signaling pathway components on d5.5pc uteri of Cripto cKO and control females. Although the level of P4 on d7.5pc and the expression of Ihh, Cox2, Hoxa10, and Hoxa11 on d5.5pc showed no difference between groups, the expression of Bmp2 and Wnt4 were significantly lower in d5.5pc nonpregnant Cripto cKO mice compared to the pregnant d5.5pc Cripto cKO and Controls. The expression of Wnt4 was also significantly lower in pregnant d5.5pc Cripto cKO compared to pregnant d5.5pc Controls. In a study by

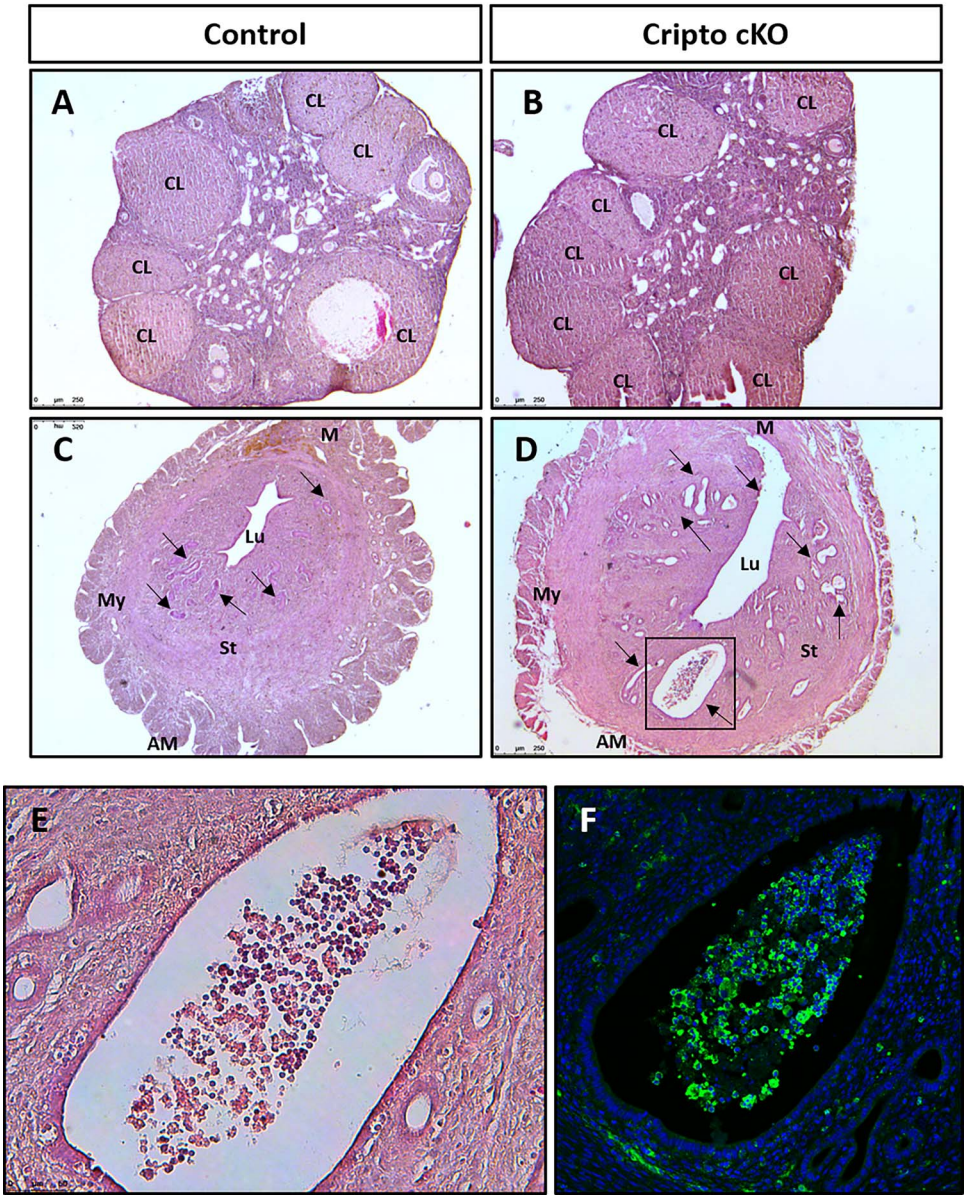

Figure 6. Abnormal histology of the uterus in older Cripto cKO females. Hematoxylin and eosin (H&E) stained sections from d3.5pc ovary (A–B) and uterus (C–D) from control and Cripto cKO females. Average number of CLs per ovary is comparable between two groups. However, in contrary to Controls, endometrial glands (arrows) are mostly distended in sections from Cripto cKO females (six out of seven Cripto cKO females) and some glandular lumens are Infiltrated by immune cells (six out of seven Cripto cKO females). (E) is higher magnification of the boxed area in (D) which show cell infiltration within a distended glandular lumen. (F) is IF staining against CD45 (green, general immune cell marker) on an adjacent serial section presented in (D) showing that those infiltrated cells are immune cells. Images are representative of ≥3 independent samples for each timepoint. AM, antimesometrial pole; CL, corpus luteum; Lu, lumen; M, mesometrial pole; My, myometrium; St, stroma. (Scale bar, A–D: 250 μm; E: 50 μm).

Farah et al. in 2017 [37] it was shown that in the uteri of porcupine cKO females in which signaling by all Wnts is disrupted, on d5.5pc the level of Wnt4 expression is significantly decreased and these females have impaired uterine decidualization. As mentioned before, Cripto enhances canonical Wnt signaling [38], therefore a possible cause for the lowered levels of Wnt4 in Cripto cKO females might be a potential decrease in canonical Wnt signaling activity.

BMP2 [10] and Wnt4 [39] which are both critical decidualization elements are suggested to be involved more in differentiation of decidual cells rather than the proliferation phase [40]. We evaluated the differentiation state of decidual cells in d5.5pc pregnant Cripto cKO females versus Controls using a staining for tissue ALP activity. Differentiated decidual cells should have a high level of ALP enzyme which results in a strong staining. Interestingly this experiment showed that decidual cell differentiation is indeed compromised in Cripto cKO females.

The Notch signaling pathway and its components such as Notch1 and Rbpj have been shown to be critical for uterine stromal decidualization [32, 33], stromal remodeling and uterine luminal closure [17]. We have seen a significant decrease in the expression of Notch1, Notch4, and Dll4 in the uteri of pregnant d5.5pc Cripto cKO compared to control females. In addition, histological analysis

during the postimplantation period, abnormal implantation crypts and failure of uterine luminal closure were frequently observed in Cripto cKO females in contrast to controls. These findings are very similar to phenotypes observed in the case of disruption of Notch signaling pathway [17]. Cripto has been shown to be implicated in enhancing of Notch signaling [34]. Impaired decidualization and uterine luminal closure process in Cripto cKO mice can therefore be the result of decreased activity of Notch signaling which in turn results in lowered expression of Notch receptors [41] leading to additional decrease in the activity of Notch signaling pathway and worsening of the condition.

An interesting finding of our study was drastic decline in fertility of Cripto cKO females by age. We concluded that this decline in fertility was not the pathological impact of repeated pregnancy failure/complications because old virgin females that never had mated before were also infertile contrary to the age-matched virgin. Further analysis showed these old Cripto cKO females are cyclic and ovulate normally, but the number of viable blastocysts retrieved from their uterus on d3.5 postcoitum is lower than control females. Abnormal histology (distended endometrial glands) and significant infiltration of immune cells into the lumen of distended uterine glands suggested an unfavorable uterine environment for blastocysts survival and subsequent implantation leading to infertility of aging Cripto cKO females.

Conclusion

We have characterized the expression pattern of Cripto during early mouse pregnancy and studied the effects of deleting Cripto in the female reproductive tract which results in subfertility in the forms of lower pregnancy rate and smaller litter size. We have also shown that the presence of defective peri-implantation uterine remodeling, decidualization, and luminal closure in Cripto cKO females are the underlying causes for their subfertility.

Although we have not shown this directly, based on findings of this study, we suggest that Cripto exerts functions in female reproduction that can be both related and independent of Nodal signaling. We have introduced a mouse model to better understand the regulation of female reproduction by TGF-β related signaling which also can be considered a good tool to study the pathogenesis of pregnancy-related issues in humans aiming toward the development of new treatments for female infertility and pregnancy complications.

Availability of data and materials

All data are incorporated into the article and its online supplementary material.

Supplementary material

Supplementary material is available at *BIOLRE* online.

References

1. Dey SK, Lim H, Das SK, Reese J, Paria BC, Daikoku T, Wang H. Molecular cues to implantation. *Endocr Rev* 2004; **25**:341–373.
2. Wang HB, Dey SK. Roadmap to embryo implantation: clues from mouse models. *Nat Rev Genet* 2006; **7**:185–199.
3. Cha JY, Sun XF, Dey SK. Mechanisms of implantation: strategies for successful pregnancy. *Nat Med* 2012; **18**:1754–1767.
4. Ayash TA, Starr LM, Dufort D. Nodal is required to maintain the uterine environment in an anti-inflammatory state during pregnancy. *Biol Reprod* 2020; **102**:1340–1350.
5. Matzuk MM, Kumar TR, Bradley A. Different phenotypes for mice deficient in either ACTIVINS or ACTIVIN receptor-type-II. *Nature* 1995; **374**:356–360.
6. Dong JW, Albertini DF, Nishimori K, Kumar TR, Lu N, Matzuk MM. Growth differentiation factor-9 is required during early ovarian folliculogenesis. *Nature* 1996; **383**:531–535.
7. Elvin JA, Clark AT, Wang P, Wolfman NM, Matzuk MM. Paracrine actions of growth differentiation factor-9 in the mammalian ovary. *Mol Endocrinol* 1999; **13**:1035–1048.
8. Brown CW, Houston-Hawkins DE, Woodruff TK, Matzuk MM. Insertion of Inhbb into the Inhba locus rescues the Inhba-null phenotype and reveals new activin functions. *Nat Genet* 2000; **25**:453–457.
9. Jorgez CJ, Klysik M, Jamin SP, Behringer RR, Matzuk MM. Granulosa cell-specific inactivation of follistatin causes female fertility defects. *Mol Endocrinol* 2004; **18**:953–967.
10. Lee KY, Jeong JW, Wang J, Ma L, Martin JF, Tsai SY, Lydon JP, DeMayo FJ. Bmp2 is critical for the murine uterine decidual response. *Mol Cell Biol* 2007; **27**:5468–5478.
11. Park CB, Dufort D. Nodal expression in the uterus of the mouse is regulated by the embryo and correlates with implantation. *Biol Reprod* 2011; **84**:1103–1110.
12. Park CB, DeMayo FJ, Lydon JP, Dufort D. NODAL in the uterus is necessary for proper placental development and maintenance of pregnancy. *Biol Reprod* 2012; **86**:194.
13. Zhao KQ, Lin HY, Zhu C, Yang X, Wang H. Maternal Smad3 deficiency compromises decidualization in mice. *J Cell Biochem* 2012; **113**:3266–3275.
14. Clementi C, Tripurani SK, Large MJ, Edson MA, Creighton CJ, Hawkins SM, Kovanci E, Kaartinen V, Lydon JP, Pangas SA, DeMayo FJ, Matzuk MM. Activin-like kinase 2 functions in peri-implantation uterine signaling in mice and humans. *PLoS Genet* 2013; **9**:e1003863.
15. Nagashima T, Li Q, Clementi C, Lydon JP, DeMayo FJ, Matzuk MM. BMPR2 is required for postimplantation uterine function and pregnancy maintenance. *J Clin Investig* 2013; **123**:2539–2550.
16. Park CB, Dufort D. NODAL signaling components regulate essential events in the establishment of pregnancy. *Reproduction* 2013; **145**: R55–R64.
17. Zhang S, Kong S, Wang B, Cheng X, Chen Y, Wu W, Wang Q, Shi J, Zhang Y, Wang S, Lu J, Lydon JP et al. Uterine Rbpj is required for embryonic-uterine orientation and decidual remodeling via notch pathway-independent and -dependent mechanisms. *Cell Res* 2014; **24**: 925–942.
18. Heba T, Park C, Dufort D. Deciphering the role of the nodal SIGNALING pathway in preterm birth. *Placenta* 2015; **36**:A59–A59.
19. Peng J, Fullerton PT Jr, Monsivais D, Clementi C, Su GH, Matzuk MM. Uterine activin-like kinase 4 regulates trophoblast development during mouse placentation. *Mol Endocrinol* 2015; **29**: 1684–1693.
20. Peng J, Monsivais D, You R, Zhong H, Pangas SA, Matzuk MM. Uterine activin receptor-like kinase 5 is crucial for blastocyst implantation and placental development. *Proc Natl Acad Sci U S A* 2015; **112**: E5098–E5107.
21. Rodriguez A, Tripurani SK, Burton JC, Clementi C, Larina I, Pangas SA. SMAD signaling is required for structural integrity of the female reproductive tract and uterine function during early pregnancy in mice. *Biol Reprod* 2016; **95**:44.
22. Ni N, Li QL. TGF beta superfamily signaling and uterine decidualization. *Reprod Biol Endocrinol* 2017; **15**:84.
23. Strizzi L, Bianco C, Normanno N, Salomon D. Cripto-1: a multifunctional modulator during embryogenesis and oncogenesis. *Oncogene* 2005; **24**:5731–5741.
24. Jin JZ, Ding JX. Cripto is required for mesoderm and endoderm cell allocation during mouse gastrulation. *Dev Biol* 2013; **381**: 170–178.

25. Ding JX, Yang L, Yan YT, Chen A, Desai N, Wynshaw-Boris A, Shen MM. Cripto is required for correct orientation of the anterior-posterior axis in the mouse embryo. *Nature* 1998; **395**:702–707.
26. Klauzinska M, Castro NP, Rangel MC, Spike BT, Gray PC, Bertolette D, Cuttitta F, Salomon D. The multifaceted role of the embryonic gene Cripto-1 in cancer, stem cells and epithelial-mesenchymal transition. *Semin Cancer Biol* 2014; **29**:51–58.
27. Papageorgiou I, Nicholls PK, Wang F, Lackmann M, Makanji Y, Salamonsen LA, Robertson DM, Harrison CA. Expression of nodal signalling components in cycling human endometrium and in endometrial cancer. *Reprod Biol Endocrinol* 2009; **7**:122.
28. Bandeira CL, Urban Borbely A, Pulcineli Vieira Francisco R, Schultz R, Zugaib M, Bevilacqua E. Tumorigenic factor CRIPTO-1 is immunolocalized in extravillous cytotrophoblast in placenta creta. *Biomed Res Int* 2014; **2014**:892856.
29. Dela Cruz C, del Puerto HL, Rocha ALL, Cavallo IK, Clarizia AD, Petraglia F, Reis FM. Expression of nodal, Cripto, SMAD3, phosphorylated SMAD3, and SMAD4 in the proliferative endometrium of women with endometriosis. *Reprod Sci* 2015; **22**:527–533.
30. Soyal SM, Mukherjee A, Lee KYS, Li J, Li H, DeMayo FJ, Lydon JP. Cre-mediated recombination in cell lineages that express the progesterone receptor. *Genesis* 2005; **41**:58–66.
31. Milligan SR, Finn CA. Minimal progesterone support required for the maintenance of pregnancy in mice. *Hum Reprod* 1997; **12**:602–607.
32. Afshar Y, Jeong JW, Roqueiro D, DeMayo F, Lydon J, Radtke F, Radnor R, Miele L, Fazleabas A. Notch1 mediates uterine stromal differentiation and is critical for complete decidualization in the mouse. *FASEB J* 2012; **26**:282–294.
33. Strug MR, Su RW, Kim TH, Mauriello A, Ticconi C, Lessey BA, Young SL, Lim JM, Jeong JW, Fazleabas AT. RBPJ mediates uterine repair in the mouse and is reduced in women with recurrent pregnancy loss. *FASEB J* 2018; **32**:2452–2466.
34. Watanabe K, Nagaoka T, Lee JM, Bianco C, Gonzales M, Castro NP, Rangel MC, Sakamoto K, Sun Y, Callahan R, Salomon DS. Enhancement of notch receptor maturation and signaling sensitivity by Cripto-1. *J Cell Biol* 2009; **187**:343–353.
35. Schier AF. Nodal Morphogens. *Cold Spring Harb Perspect Biol* 2009; **1**:a003459.
36. Liu G, Lin H, Zhang X, Li Q, Wang H, Qian D, Ni J, Zhu C. Expression of Smad2 and Smad4 in mouse uterus during the oestrous cycle and early pregnancy. *Placenta* 2004; **25**:530–537.
37. Farah O, Biechele S, Rossant J, Dufort D. Regulation of porcupine-dependent Wnt signaling is essential for uterine development and function. *Reproduction* 2018; **155**:93–102.
38. Nagaoka T, Karasawa H, Turbyville T, Rangel MC, Castro NP, Gonzales M, Baker A, Seno M, Lockett S, Greer YE, Rubin JS, Salomon DS et al. Cripto-1 enhances the canonical Wnt/beta-catenin signaling pathway by binding to LRP5 and LRP6 co-receptors. *Cell Signal* 2013; **25**: 178–189.
39. Franco HL, Dai D, Lee KY, Rubel CA, Roop D, Boerboom D, Jeong JW, Lydon JP, Bagchi IC, Bagchi MK, DeMayo FJ. WNT4 is a key regulator of normal postnatal uterine development and progesterone signaling during embryo implantation and decidualization in the mouse. *FASEB J* 2011; **25**:1176–1187.
40. Ramathal CY, Bagchi I, Taylor R, Bagchi M. Endometrial Decidualization: Of mice and men. *Semin Reprod Med* 2010; **28**:17–26.
41. Artavanis-Tsakonas S, Rand MD, Lake RJ. Notch signaling: Cell fate control and signal integration in development. *Science* 1999; **284**: 770–776.